

Rhenium Polyhydride Complexes Containing PhP(CH₂CH₂CH₂PCy₂)₂ (Cytpp): Protonation, Insertion, and Ligand Substitution Reactions of ReH₅(Cytpp) and Structural Characterization of ReH₅(Cytpp) and [ReH₄(η²-H₂)(Cytpp)]SbF₆

Youhyuk Kim,[†] Haibin Deng,^{‡,§} Judith C. Gallucci,[‡] and Andrew Wojcicki^{*,‡}

Departments of Chemistry, The Ohio State University, Columbus Ohio 43210, and Dankook University, 29 Anseo Dong, Cheonan, Choongnam 330-714, South Korea

Received March 13, 1996[⊗]

Several new polyhydride complexes of rhenium containing the tridentate phosphine PhP(CH₂CH₂CH₂PCy₂)₂ (Cytpp) were synthesized and characterized by ¹H and ³¹P{¹H} NMR and IR spectroscopy. The solid state structure of the previously reported ReH₅(Cytpp) (**1**) was determined by X-ray crystallography. **1** crystallizes in the space group *P2₁/m* with the following unit cell parameters: *a* = 8.582(2) Å, *b* = 19.690(2) Å, *c* = 10.800(2) Å, β = 95.57(1)°, and *Z* = 2. The molecule adopts a classical polyhydride, triangulated dodecahedral structure, with the three phosphorus atoms and one hydrogen atom occupying the B sites, and the remaining hydrogen atoms occupying the A sites. **1** is protonated by HSBF₆ (or HBF₄) to yield [ReH₄(η²-H₂)(Cytpp)]SbF₆ (**3**), which was shown by X-ray diffraction techniques (space group *P1̄*, unit cell parameters: *a* = 9.874(2) Å, *b* = 14.242(4) Å, *c* = 16.198(2) Å, α = 99.12(2)°, β = 98.85(2)°, γ = 109.42(2)°, and *Z* = 2) to contain a nonclassical polyhydride cation with a triangulated dodecahedral structure in the solid. The same structure is suggested in solution by ¹H NMR data (including *T*₁ measurements). **3** is inert to loss of H₂ and is unaffected by CO, *t*-BuNC, and P(OMe)₃ at room temperature. In contrast, **1** reacts with a variety of reagents to afford classical tetrahydride complexes which are thought also to possess a triangulated dodecahedral structure, with the hydrogens in the A sites, from spectroscopic evidence. Accordingly, CS₂, *p*-O₂NC₆H₄NCS, and EtOC(O)NCS (X=C=S) insert into an Re–H bond to yield ReH₄(SCH=X)(Cytpp) (**5–7**, respectively). MeI cleaves one Re–H bond to afford ReH₄I(Cytpp) (**8**), and [C₇H₇]BF₄ abstracts hydride in the presence of MeCN, *t*-BuNC, CyNC, or P(OMe)₃ (L) to give [ReH₄L(Cytpp)]BF₄ (**9–12**, respectively). A related pentahydride, ReH₅(ttp) (**2**, ttp = PhP(CH₂CH₂CH₂PPh₂)₂), also reacts with HSBF₆ to yield [ReH₆(ttp)]SbF₆ (**4**), which appears to be a nonclassical polyhydride in solution by *T*₁ measurements.

Introduction

Transition-metal polyhydride complexes have received considerable recent attention because of their diverse chemistry and unusual structural properties, including possible presence of η²-H₂ ligands.^{1–6} Many of the polyhydride complexes studied contain ancillary monodentate and bidentate phosphine ligands. In contrast, related complexes with triphosphine ligands have been little investigated.⁷ Yet the use of tridentate phosphines instead of similar monodentate phosphines may lead to several desirable properties,⁸ such as increased stability to ligand

dissociation and slower rates for the hydride fluxional processes.^{7d–f}

Rhenium forms a large number of polyhydride phosphine complexes,^{1–6,9} but few of them contain tridentate phosphine ligands.^{7d,f,g} Recently we reported the synthesis of ReH₅(Cytpp) (**1**, Cytpp = PhP(CH₂CH₂CH₂PCy₂)₂) and ReH₅(ttp) (**2**, ttp = PhP(CH₂CH₂CH₂PPh₂)₂) and reactions of these complexes with RO₂CCH=CHCO₂R.^{7g} We also reported in preliminary communications the protonation of **1** to yield [ReH₄(η²-H₂)(Cytpp)]⁺ (**3**)^{7f} and the reaction of the latter with acetone to produce [ReH₂(O)(Cytpp)]⁺.¹⁰ Concurrently with our studies, Crabtree and Luo synthesized and characterized by spectroscopic means the related complexes ReH₅(etp) and [ReH₆(etp)]⁺ (etp = PhP(CH₂CH₂-PPh₂)₂), the latter being near the classical/nonclassical borderline, i.e. ReH₆/ReH₄(η²-H₂).^{7d}

As part of our continuing investigations into the chemistry of rhenium hydride complexes containing tridentate phosphine

* To whom correspondence should be addressed.

[†] Dankook University.

[‡] The Ohio State University.

[§] Deceased.

[⊗] Abstract published in *Advance ACS Abstracts*, October 15, 1996.

- (1) Kubas, G. J. *Acc. Chem. Res.* **1988**, *21*, 120.
- (2) Crabtree, R. H.; Hamilton, D. G. *Adv. Organomet. Chem.* **1988**, *28*, 299.
- (3) Crabtree, R. H. *Acc. Chem. Res.* **1990**, *23*, 95.
- (4) Desrosiers, P. J.; Cai, L.; Lin, Z.; Richards, R.; Halpern, J. *J. Am. Chem. Soc.* **1991**, *113*, 4173.
- (5) Morris, R. H.; Jessop, P. G. *Coord. Chem. Rev.* **1991**, *121*, 155.
- (6) Heinekey, D. M.; Oldham, W. J., Jr. *Chem. Rev.* **1993**, *93*, 913.
- (7) Selected examples: (a) Bianchini, C.; Peruzzini, M.; Zanobini, F. *J. Organomet. Chem.* **1988**, *354*, C19. (b) Bianchini, C.; Perez, P. J.; Peruzzini, M.; Zanobini, F.; Vacca, A. *Inorg. Chem.* **1991**, *30*, 279. (c) Bianchini, C.; Peruzzini, M.; Polo, A.; Vacca, A.; Zanobini, F. *Gazz. Chim. Ital.* **1991**, *121*, 543. (d) Luo, X.-L.; Crabtree, R. H. *J. Chem. Soc., Dalton Trans.* **1991**, 587. (e) Michos, D.; Luo, X.-L.; Fallner, J. W.; Crabtree, R. H. *Inorg. Chem.* **1993**, *32*, 1370. (f) Kim, Y.; Deng, H.; Meek, D. W.; Wojcicki, A. *J. Am. Chem. Soc.* **1990**, *112*, 2798. (g) Kim, Y.; Gallucci, J.; Wojcicki, A. *Organometallics* **1992**, *11*, 1963.

- (8) Selected examples: (a) Mason, R.; Meek, D. W. *Angew. Chem., Int. Ed. Engl.* **1978**, *17*, 183. (b) Meek, D. W.; Mazanec, T. J. *Acc. Chem. Res.* **1981**, *14*, 266.
- (9) Other selected examples: (a) Emge, T. J.; Koetzel, T. F.; Bruno, J. W.; Caulton, K. G. *Inorg. Chem.* **1984**, *23*, 4012. (b) Howard, J. A. K.; Mason, S. A.; Johnson, O.; Diamon, I. C.; Crennell, S.; Keller, P. A.; Spencer, J. L. *J. Chem. Soc., Chem. Commun.* **1988**, 1502. (c) Cotton, F. A.; Luck, R. L. *Inorg. Chem.* **1989**, *28*, 2181. (d) Cotton, F. A.; Luck, R. L.; Root, D. R.; Walton, R. A. *Inorg. Chem.* **1990**, *29*, 43. (e) Earl, K. A.; Jia, G.; Maltby, P. A.; Morris, R. H. *J. Am. Chem. Soc.* **1991**, *113*, 3027. (f) Haynes, G. R.; Martin, R. L.; Hay, P. J. *J. Am. Chem. Soc.* **1992**, *114*, 28. (g) Loza, M. L.; de Gala, S. R.; Crabtree, R. H. *Inorg. Chem.* **1994**, *33*, 5073. (h) Heinekey, D. M.; Liegeois, A.; van Roon, M. *J. Am. Chem. Soc.* **1994**, *116*, 8388.
- (10) Kim, Y.; Gallucci, J.; Wojcicki, A. *J. Am. Chem. Soc.* **1990**, *112*, 8600.

ligands, we have examined the reactivity of **1** toward the heterocumulenes $X=C=S$ where $X = S$, $p\text{-O}_2\text{NC}_6\text{H}_4\text{N}$, and EtOC(O)N , toward MeI , and toward $[\text{C}_7\text{H}_7]\text{BF}_4$ in the presence of several ligands L . Reported here are the results of this study, as well as the details of the structural and spectroscopic investigations of **1** and **3**. Also included in this paper are the synthesis and spectroscopic characterization of the ttp analogue of **3**, $[\text{ReH}_6(\text{ttp})]\text{SbF}_6$ (**4**). (This formula will be used throughout the paper, since evidence for a nonclassical structure of complex **4** is incomplete.)

Experimental Section

General Procedures. All reactions and sample manipulations were conducted under an atmosphere of Ar by use of standard procedures.¹¹ Solvents were dried,¹² distilled under Ar, and degassed before use. Elemental analyses were performed by M-H-W Laboratories, Phoenix, AZ. Infrared (IR) spectra were recorded on a Perkin-Elmer Model 283B grating spectrophotometer as Nujol mulls between KBr plates and were calibrated with polystyrene. NMR spectra were collected on a Bruker AM-250 spectrometer. ^1H chemical shifts were measured with the residual solvent resonance as reference. ^{31}P chemical shifts were referenced to external 85% H_3PO_4 . T_1 measurements were carried out by the inversion–recovery method using a standard $180^\circ - \tau - 90^\circ$ pulse sequence.

Materials. Reagents were obtained from commercial sources and used as received, except as noted below. The complexes $\text{ReH}_5(\text{Cytpp})$ (**1**) and $\text{ReH}_5(\text{ttp})$ (**2**) were prepared by the literature procedures.^{7e} The synthetic methods for the tridentate phosphine ligands Cytpp ($\text{PhP}(\text{CH}_2\text{CH}_2\text{CH}_2\text{C}_6\text{H}_4)_2$) and ttp ($\text{PhP}(\text{CH}_2\text{CH}_2\text{CH}_2\text{PPh}_2)_2$) were essentially those reported by Meek and co-workers.¹³

Preparation of $[\text{ReH}_4(\eta^2\text{-H}_2)(\text{Cytpp})]\text{SbF}_6$ (3**).** To a solution of $\text{ReH}_5(\text{Cytpp})$ (**1**) (1.00 g, 1.29 mmol) in 50 mL of benzene was added an excess of 65% aqueous HSbF_6 (1.5 mL, 2.2 mmol), and the mixture was stirred for 30 min at room temperature. The volume of the solution was reduced to ca. 3 mL under reduced pressure, and 30 mL of Et_2O was added to give a white precipitate. The powder was collected on a filter frit, washed with a small amount of Et_2O , and dried under vacuum overnight. Yield: 1.21 g (92%). Anal. Calcd for $\text{C}_{36}\text{H}_{67}\text{F}_6\text{P}_3\text{ReSb}$: C, 42.61; H, 6.65. Found: C, 42.73; H, 6.68.

By using HBF_4 in place of HSbF_6 , $[\text{ReH}_4(\eta^2\text{-H}_2)(\text{Cytpp})]\text{BF}_4$ was isolated in 88% yield. Anal. Calcd for $\text{C}_{36}\text{H}_{67}\text{BF}_4\text{P}_3\text{Re}$: C, 49.94; H, 7.80; P, 10.73. Found: C, 49.93; H, 7.66; P, 10.81.

Preparation of $[\text{ReH}_6(\text{ttp})]\text{SbF}_6$ (4**).** To a solution of $\text{ReH}_5(\text{ttp})$ (**2**) (0.20 g, 0.27 mmol) in 50 mL of benzene was added an excess of 65% aqueous HSbF_6 (1.5 mL, 2.2 mmol), and the mixture was stirred for 30 min at room temperature. The solution was concentrated to ca. 2 mL under reduced pressure, and 20 mL of Et_2O was added to give a tan precipitate. The solid was collected on a filter frit, washed with a small amount of Et_2O , and dried under vacuum. Yield: 0.20 g (74%).

Reaction of $\text{ReH}_5(\text{Cytpp})$ (1**) with CS_2 .** A benzene solution (25 mL) of **1** (0.10 g, 0.13 mmol) and excess CS_2 (0.10 mL, 2.1 mmol) was stirred for 2 h at room temperature. The solution was then evaporated to dryness, 10 mL of Et_2O was added, and the mixture was again stirred for several hours. The resultant yellow solid was collected on a filter frit, washed with Et_2O , and dried under vacuum overnight. Yield of $\text{ReH}_4(\text{SCH}=\text{S})(\text{Cytpp})$ (**5**): 0.092 g (82%). Anal. Calcd for $\text{C}_{37}\text{H}_{66}\text{P}_3\text{S}_2\text{Re}$: C, 52.03; H, 7.79; S, 7.51. Found: C, 52.37; H, 7.69; S, 7.77.

Reaction of $\text{ReH}_5(\text{Cytpp})$ (1**) with $p\text{-O}_2\text{NC}_6\text{H}_5\text{NCS}$.** A benzene solution (25 mL) of **1** (0.10 g, 0.13 mmol) and excess $p\text{-O}_2\text{NC}_6\text{H}_4\text{NCS}$ (0.10 g, 0.55 mmol) was stirred for 30 min at room temperature. The solvent was removed under vacuum, and 10 mL of Et_2O was added to the dark violet residue. After trituration, the powder was collected on a filter frit, washed with a small amount of Et_2O , and dried under

vacuum overnight. Yield of $\text{ReH}_4(\text{SCH}=\text{NC}_6\text{H}_4\text{NO}_2\text{-}p)(\text{Cytpp})$ (**6**): 0.083 g (67%). Anal. Calcd for $\text{C}_{43}\text{H}_{70}\text{N}_2\text{O}_2\text{P}_3\text{ReS}$: C, 53.90; H, 7.36; N, 2.92; S, 3.35. Found: C, 54.09; H, 7.29; N, 2.88; S, 3.46.

Reaction of $\text{ReH}_5(\text{Cytpp})$ (1**) with EtOC(O)NCS .** A benzene solution (25 mL) of **1** (0.10 g, 0.13 mmol) and excess EtOC(O)NCS (0.50 mL, 4.2 mmol) was stirred for 30 min at room temperature to give a reddish brown solution. The solvent was removed under vacuum, and 15 mL of Et_2O was added to the rust-colored residue. After trituration, the solid was collected on a filter frit, washed with a small amount of Et_2O , and dried under vacuum overnight. Yield of $\text{ReH}_4(\text{SCH}=\text{NC(O)OEt})(\text{Cytpp})$ (**7**): 0.10 g (83%). Anal. Calcd for $\text{C}_{40}\text{H}_{71}\text{NO}_2\text{P}_3\text{ReS}$: C, 52.84; H, 7.87. Found: C, 52.78; H, 7.69.

Reaction of $\text{ReH}_5(\text{Cytpp})$ (1**) with MeI .** To a solution of **1** (0.10 g, 0.13 mmol) in 25 mL of benzene was added excess MeI (0.10 mL, 1.6 mmol), and the mixture was stirred for 45 min at room temperature to give a white precipitate. The solution was concentrated to ca. 5 mL and treated with 10 mL of Et_2O to induce the formation of additional solid. The white powder was collected on a filter frit, washed with a small amount of Et_2O , and dried under vacuum. It is insoluble in benzene and acetone, but slightly soluble in CH_2Cl_2 . Yield of $\text{ReH}_4\text{I}(\text{Cytpp})$ (**8**): 0.11 g (92%). Anal. Calcd for $\text{C}_{36}\text{H}_{67}\text{IP}_3\text{Re}$: C, 47.83; H, 7.25; I, 14.04; P, 10.28. Found: C, 47.66; H, 7.15; I, 14.29; P, 10.31.

Reaction of $\text{ReH}_5(\text{Cytpp})$ (1**) with $[\text{C}_7\text{H}_7]\text{BF}_4$ in Presence of MeCN .** A solution of **1** (0.10 g, 0.13 mmol) and excess MeCN (1.0 mL, 19 mmol) in 25 mL of benzene was treated with $[\text{C}_7\text{H}_7]\text{BF}_4$, also in excess (ca. 0.10 g, 0.56 mmol), and the contents were stirred for 2 h at room temperature. The reaction mixture was filtered through a frit to remove unreacted $[\text{C}_7\text{H}_7]\text{BF}_4$. The volume of the filtrate was reduced to ca. 3 mL, and 10 mL of Et_2O was added to induce the precipitation of a white solid. The solid was collected on a filter frit, washed with a small amount of Et_2O , and dried under vacuum. Yield of $[\text{ReH}_4(\text{MeCN})(\text{Cytpp})]\text{BF}_4$ (**9**): 0.094 g (77%). Anal. Calcd for $\text{C}_{38}\text{H}_{68}\text{BF}_4\text{NP}_3\text{Re}$: C, 50.44; H, 7.57; N, 1.55. Found: C, 50.26; H, 7.71; N, 1.52.

Reaction of $\text{ReH}_5(\text{Cytpp})$ (1**) with $[\text{C}_7\text{H}_7]\text{BF}_4$ in Presence of $t\text{-BuNC}$.** A solution of **1** (0.10 g, 0.13 g) and excess $t\text{-BuNC}$ (ca. 0.050 mL, 0.44 mmol) in 25 mL of benzene was treated with $t\text{-BuNC}$, also in excess (0.10 g, 0.56 mmol). The mixture was stirred for 2 h at room temperature and then filtered through a frit. The filtrate was evaporated to dryness, and the residue was treated with 10 mL of Et_2O . After trituration, the white solid was collected on a filter frit, washed with a small amount of Et_2O , and dried under vacuum. Yield of $[\text{ReH}_4(t\text{-BuNC})(\text{Cytpp})]\text{BF}_4$ (**10**): 0.10 g (81%). Anal. Calcd for $\text{C}_{41}\text{H}_{74}\text{BF}_4\text{NP}_3\text{Re}$: C, 52.00; H, 7.88; N, 1.48. Found: C, 52.17; H, 7.90; N, 1.49.

Reaction of $\text{ReH}_5(\text{Cytpp})$ (1**) with $[\text{C}_7\text{H}_7]\text{BF}_4$ in Presence of CyNC .** The procedure was identical with that for **10**, except that CyNC (0.050 mL) was used in place of $t\text{-BuNC}$. Yield of $[\text{ReH}_4(\text{CyNC})(\text{Cytpp})]\text{BF}_4$ (**11**): 0.070 g (56%). Anal. Calcd for $\text{C}_{43}\text{H}_{76}\text{BF}_4\text{NP}_3\text{Re}$: C, 53.08; H, 7.87; N, 1.44. Found: C, 52.90; H, 7.66; N, 1.45.

Reaction of $\text{ReH}_5(\text{Cytpp})$ (1**) with $[\text{C}_7\text{H}_7]\text{BF}_4$ in Presence of P(OMe)_3 .** The procedure was identical with that for **10**, except that P(OMe)_3 (0.050 mL, 0.42 mmol) was used in place of $t\text{-BuNC}$. Yield of $[\text{ReH}_4(\text{P(OMe)}_3)(\text{Cytpp})]\text{BF}_4$ (**12**): 0.072 g (55%). Anal. Calcd for $\text{C}_{39}\text{H}_{74}\text{BF}_4\text{O}_3\text{P}_4\text{Re}$: C, 47.42; H, 7.55; P, 12.54. Found: C, 47.52; H, 7.45; P, 12.66.

X-ray Data Collection and Refinement of the Structure of $\text{ReH}_5(\text{Cytpp})$ (1**).** Crystals for X-ray diffraction were obtained by slow evaporation of the solvent from a saturated benzene solution under a flow of argon. The crystal used for data collection was clear, light tan in color with a rectangular rod-like morphology. Diffraction data were collected for compounds **1** and **3** as summarized in Table 1. Examination of the diffraction pattern on a Rigaku AFC5S diffractometer showed a monoclinic crystal system with systematic absences: $0k0$, $k = 2n + 1$. The space group possibilities are limited to $P2_1$ or $P2_1/m$. The cell constants were determined at room temperature by a least-squares fit of the diffractometer setting angles for 25 reflections in the 2θ range $29\text{--}30^\circ$ and with $\text{Mo K}\alpha$ radiation ($\lambda(\text{K}\alpha) = 0.71069 \text{ \AA}$).

Intensities were measured by the $\omega\text{--}2\theta$ scan method. Six standard reflections measured after every 150 reflections indicated that the crystal

(11) Shriver, D. F.; Drezdson, M. A. *The Manipulation of Air-Sensitive Compounds*, 2nd ed.; Wiley: New York, 1986.

(12) Perrin, D. D.; Amarego, W. L. F.; Perrin, D. R. *Purification of Laboratory Chemicals*; Pergamon Press: Oxford, U.K., 1966.

(13) Uriarte, R.; Mazanec, T. J.; Tau, K. D.; Meek, D. W. *Inorg. Chem.* **1980**, *19*, 79.

Table 1. Crystallographic Data for Complexes **1** and **3**

	1	3
chem formula	C ₃₆ H ₆₆ P ₃ Re	C ₃₆ H ₆₇ F ₆ P ₃ ReSb
fw	778.05	1014.80
space group	<i>P2</i> ₁ / <i>m</i>	<i>P</i> $\bar{1}$
<i>a</i> , Å	8.582(2)	9.874(2)
<i>b</i> , Å	19.690(2)	14.242(4)
<i>c</i> , Å	10.800(2)	16.198(2)
α , deg		99.12(2)
β , deg	95.57(1)	98.85(2)
γ , deg		109.42(2)
<i>V</i> , Å ³	1816	2068
<i>Z</i>	2	2
<i>D</i> _{calcd} , g cm ⁻³	1.42	1.63
μ , cm ⁻¹	35.42	37.85
temp, °C	23	-50
transm coeff	0.692–1.000	0.564–0.999
<i>R</i> (<i>F</i>) ^a	0.022	0.022
<i>R</i> _w (<i>F</i>) ^b	0.027	0.032

^a $R(F) = \frac{\sum ||F_o| - |F_c||}{\sum |F_o|}$, ^b $R_w(F) = \frac{[\sum w(|F_o| - |F_c|)]^2}{\sum w|F_o|^2}^{1/2}$ with $w = 1/\sigma^2(F_o)$.

was stable during the data collection. Data reduction and all additional calculations were done with the TEXSAN package of crystallographic programs.¹⁴

The structure was solved and successfully refined in *P2*₁/*m*. With two molecules in the unit cell, the molecule is required to contain a crystallographic mirror plane. The position of the Re atom was located from a Patterson map. The Re atom was then used as a phasing model in DIRDIF,¹⁵ and most of the remainder of the atoms in the asymmetric unit appeared on the resulting electron density map, with the exception of six carbon atoms. The positions of these missing atoms were obtained by standard Fourier methods. Full-matrix least-squares isotropic refinement converged at an *R* value of 0.066 for those reflections with $F_o^2 > 3\sigma(F_o^2)$. At this point an absorption correction based on ψ scans¹⁶ was applied to the data set, and subsequent isotropic refinement converged at *R* = 0.042. After one cycle of anisotropic refinement, all of the hydrogen atoms, including the four unique hydrides, were located on a difference electron density map. These hydride positions were also evident in a difference Fourier map calculated with low angle data ($2\theta_{\max} = 35^\circ$). There are five hydride H atoms bonded to the Re atom. The crystallographic mirror plane which passes through the molecule reduces this set of 5 to 4 unique hydrides: H1, H2, H3, and H4. H1, H2, and H3 lie on the mirror plane. H4 lies off the mirror plane, and its symmetry-generated position is labeled as H4', which is the fifth hydride atom. The four hydrogen atoms bonded to rhenium were initially fixed at their positions from the difference map, but in the final stages of refinement they were refined isotropically. The other hydrogen atoms were included in the model as fixed contributions in their calculated positions with the assumptions: C–H = 0.98 Å and $B_H = 1.2B_{C(\text{eq})}$ (attached carbon atom). The final refinement cycle resulted in agreement indices of *R* = 0.022 and *R*_w = 0.027 based on the 3721 reflections with $F_o^2 > 3\sigma(F_o^2)$ and the 206 variables. One reflection was removed from the data set because of uneven backgrounds: (1,19,1). The maximum and minimum peaks in the final difference electron density map are +0.52 and -0.61 e/Å³. Scattering factors for neutral atoms, including terms for anomalous scattering, were used.¹⁷ All full-matrix least-squares refinements were based on *F* so that the function minimized in least-squares is $\sum w(|F_o| - |F_c|)^2$ with $w = 1/\sigma^2(F_o)$.

X-ray Data Collection and Refinement of the Structure of [ReH₄(η^2 -H₂)(Cyttp)]SbF₆ (3). Crystals for X-ray diffraction were

(14) TEXSAN, TEXRAY Structure Analysis Package, Version 2.1, Molecular Structure Corp., College Station, TX, 1987.

(15) Parthasarathi, V.; Beurskens, P. T.; Slot, H. J. B. *Acta Crystallogr.* **1983**, A39, 860.

(16) North, A. C. T.; Phillips, D. C.; Mathews, F. S. *Acta Crystallogr.* **1968**, A24, 351.

(17) Scattering factors for the non-hydrogen atoms and anomalous dispersion terms are from: *International Tables for X-ray Crystallography*; Kynoch Press: Birmingham, U.K., 1974; Vol. IV, pp 71, 148. The scattering factor for the hydrogen atom is from: Stewart, R. F.; Davidson, E. R.; Simpson, W. T. *J. Chem. Phys.* **1965**, 42, 3175.

obtained by slowly evaporating solvents from a saturated solution of CH₂Cl₂/MeOH under a flow of argon. A colorless crystal was glued at the tip of a glass fiber and mounted on a Enraf Nonius CAD4 diffractometer. All data were collected at 223 K with graphite monochromated MoK α radiation. The unit cell dimensions were obtained from the setting angles of 25 reflections with $24^\circ < 2\theta < 30^\circ$. The space group choices are restricted to *P1* and *P* $\bar{1}$.

The intensity data were collected in the ω - 2θ scan mode. Three standard reflections were monitored every 3 h of X-ray exposure, and they indicated a slight linear crystal decay (-6.4%). All calculations were performed with the SDP package.¹⁸ The data were corrected for decay and for absorption by the ψ scan method.¹⁶ The structure was solved by the combination of direct methods (MULTAN 11/82)¹⁹ and Fourier synthesis in space group *P* $\bar{1}$.

Full-matrix least-squares refinements were carried out with anisotropic thermal parameters for the non-hydrogen atoms. The hydrogen atoms attached to carbons were included in the refined structure at calculated positions with C–H = 0.98 Å and $B_H = 1.2B_{C(\text{eq})}$. A difference electron density map calculated with all the atoms in the model except for the hydrogens bonded to Re shows the following peak heights: the top two peaks at 1.05 and 0.84 e/Å³ are noise peaks near Re, while the next seven peaks at 0.79–0.50 e/Å³ correspond to H2, H5, H1, noise near Sb, H3, noise near F3, and H6, respectively. A difference electron density map for the same model calculated with a $(\sin \theta)/\lambda$ cutoff of 0.42 Å⁻¹ results in the top six peaks corresponding to H4, H1, H2, H5, noise near Re, and H6, respectively, within the range 0.79–0.38 e/Å³; contour plots of various planes show compact peaks for H1, H2, H5, and H6 but a large, diffuse peak for H4. The area for this large peak can incorporate both H3 and H4; this would explain why H3 is located in the map calculated with no $(\sin \theta)/\lambda$ cutoff, while H4 appears in the 0.42 Å⁻¹ map. To further investigate this large peak, H1, H2, H5, and H6 were added to the model and refined isotropically. A contoured difference electron density map for a plane parallel to the plane defined by Re, P2, and P3 and displaced from it by 1.60 Å shows two peaks about 1.0 Å apart. This is the region where the large, diffuse peak previously appeared when no hydrides were in the model and is here interpreted as the η^2 -H₂ ligand (H3–H4) (cf. Figure 1).

The final refinement cycle for 7982 unique observations with $F_o^2 > 3\sigma(F_o^2)$ and 449 variable parameters resulted in the residual factors of *R* = 0.022 and *R*_w = 0.032. The maximum and minimum peaks in the final difference Fourier map were +0.75 and -0.89 e/Å³, respectively.

Results and Discussion

Spectroscopic Properties of ReH₅(triphos) (1, 2). The complexes ReH₅(triphos) (**1**, triphos = Cyttp; **2**, triphos = ttp) were prepared by reaction of ReCl₃(PMePh₂)₃ with triphos followed by treatment of products ReCl₃(triphos) with an excess of NaBH₄. These syntheses were described in detail in our earlier paper.^{7g} We now report the characterization of both complexes by spectroscopic methods and of **1** by X-ray diffraction techniques.

Selected ¹H and ³¹P{¹H} NMR data for **1** and **2** are presented in Table 2. In the ¹H NMR spectra, the five hydrogens bonded to rhenium are fluxional and appear as a triplet of doublets owing to the different coupling to the wing and the central phosphorus atoms. A similar spectrum was obtained for the related complex ReH₅(etp) (etp = PhP(CH₂CH₂PPh₂)₂) by Crabtree and Luo.^{7d} In contrast, the monophosphine analogues of **1** and **2**, ReH₅(PR₃)₃ (R₃ = Ph₃,²⁰ MePh₂,^{9a} Me₂Ph,²¹ EtPh₂,²⁰ EtPh²⁰) and ReH₅(PR₃)₂(PR'₃)²⁰ (R₃ = Et₂Ph, R'₃ =

(18) SDP, Structure Determination Package. B. A. Frenz and Associates, Inc.; College Station, TX, and Enraf-Nonius, Delft, Holland, 1982.

(19) Multan 11/82, A System of Computer Programs for the Automatic Solution of Crystal Structures from X-ray Diffraction Data. Hull, S. E.; Lessinger, L.; Germain, G.; Declercq, J.-P.; Wolfson, M. M. University of York, York, U.K., 1982.

(20) Chatt, J.; Coffey, R. S. *J. Chem. Soc. A.* **1969**, 1963.

(21) Douglas, P. G.; Shaw, B. L. *Inorg. Synth.* **1978**, 17, 64.

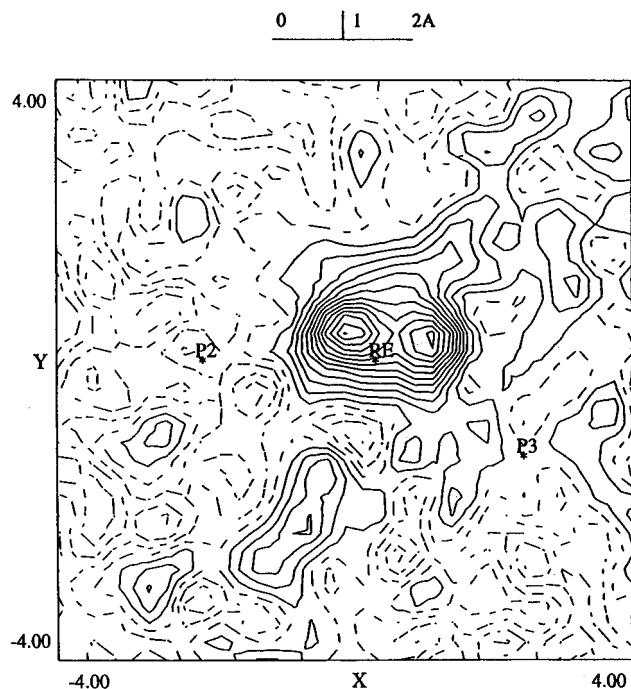


Figure 1. Difference electron density map calculated for a plane which is parallel to the plane defined by Re, P2, and P3 and displaced from it by 1.60 Å. The contours are drawn at levels of $0.05 e/\text{Å}^3$. Positive regions are contoured with solid lines, and negative regions are represented by dashed lines. The model used for this map consists of all the atoms except for H3 and H4. The positive peaks which lie on either side of Re correspond to H3 and H4.

Ph₃) show a symmetrical quartet owing to the equivalence of the three phosphorus atoms at room temperature on the NMR time scale. When the solution of **1** is cooled to 183 K, the doublet of triplets becomes a broad, featureless peak to indicate that the fluxional behavior of the hydrides has not been completely arrested. The $^{31}\text{P}\{^1\text{H}\}$ NMR spectra of **1** and **2** show a doublet for the equivalent wing phosphorus atoms and a triplet for the central phosphorus atom. In the IR spectrum of **1** in Nujol mull, $\nu(\text{ReH})$ absorptions are observed at 1995 (w), 1900 (m), 1850 (sh), and 1835 (s) cm^{-1} . These data are similar to those reported for $\text{ReH}_5(\text{PR}_3)_3$.^{20,21}

Description of the Structure of $\text{ReH}_5(\text{Cytpp})$ (1**).** The structure of **1** in the solid is presented in Figure 2, and selected bond distances and angles are listed in Table 3. The coordination geometry about the rhenium center in **1** is that of a triangulated dodecahedron, and this polyhedral arrangement is shown in Figure 3. Two orthogonal trapezoidal planes (A_2B_2)²² are characteristic of the idealized triangulated dodecahedron. For **1**, both trapezoidal planes are truly planar and orthogonal to each other. One of these planes contains the atoms P1, H1, H2, and H3 and is coincident with a crystallographic mirror plane, which also includes the Re atom and the phenyl ring. As a result, the second trapezoidal plane (P2, H4, H4', P2') is required to be exactly planar and orthogonal to the first one.

There are two types of hydride ligand about the Re center: the four hydrides (H1, H2, H4, and H4') that occupy four-neighbor A sites and one hydride (H3) that occupies a five-neighbor B site. The three phosphorus atoms of the Cytpp ligand take up the remaining B sites as shown in Figure 3. A similar distribution of hydrogen and phosphorus atoms in triangulated dodecahedral structures has been found for $\text{ReH}_5(\text{PMePh}_2)_3$.^{9a}

by neutron diffraction methods and for $\text{ReH}_5(\text{PPh}_3)_3$ ²³ and $[(\text{ReH}_5(\text{PMePh}_2)_3)_2\text{Cu}]^+$ ²⁴ by X-ray diffraction methods. Another eight-coordinate complex, $\text{MoH}_4(\text{PMePh}_2)_4$ ²⁵ shows (X-ray diffraction) a symmetrical arrangement of A-site hydrides and B-site phosphines.

The mean Re–P bond distance of **1** (2.380 Å) falls in the same range as that of the monophosphine analogues $\text{ReH}_5(\text{PMePh}_2)_3$ (2.38(6) Å)^{9a} and $\text{ReH}_5(\text{PPh}_3)_3$ (2.393(2) Å).²³ The Re–P1 bond distance (2.374(1) Å) is shorter than Re–P2 (or Re–P2') (2.3828(7) Å), in contrast to the corresponding values for $\text{ReH}_5(\text{PMePh}_2)_3$ (2.397(3) vs 2.373(6) Å) and $\text{ReH}_5(\text{PPh}_3)_3$ (2.403(2) vs 2.397(2) Å). The P–Re–P bond angles in **1** give the characteristic one large/two small ($151.80(4)^\circ$, $95.10(2)^\circ$, $95.10(2)^\circ$) pattern of a triangulated dodecahedral structure, as found in $\text{ReH}_5(\text{PMePh}_2)_3$ ($146.5(2)$, $103.4(2)$, $99.0(2)^\circ$ and $148.0(2)$, $101.6(2)$, $100.9(2)^\circ$) for two independent molecules in the unit cell,^{9a} $\text{ReH}_5(\text{PMe}_2\text{Ph})_3$ ($149.5(2)$, $101.9(2)$, $99.8(2)^\circ$),²⁶ and $\text{ReH}_5(\text{PPh}_3)_3$ ($133.28(7)$, $108.38(7)$, $107.43(7)^\circ$).²² The relatively small values of the P1–Re–P2 and P1–Re–P2' angles of **1** compared to those of the monophosphine analogues are presumably due to the constraining nature of the chelating Cytpp ligand. In **1**, the Re–H bond lengths range from 1.53(4) to 1.70(5) Å (1.60 Å mean). For comparison, neutron diffraction studies showed Re–H distances of 1.688(5) Å in $\text{ReH}_5(\text{PMePh}_2)_3$,^{9a} 1.68(1) Å in K_2ReH_9 ,²⁷ and 1.669(7) Å (for terminal hydrides) in $\text{Re}_2\text{H}_8(\text{PET}_2\text{Ph})_4$.²⁸ The shortest H···H interatomic distance in **1** (H4···H4' 1.61(7) Å, cf. Supporting Information) is too long to be associated with an $\eta^2\text{-H}_2$ bond.

Protonation of $\text{ReH}_5(\text{triphos})$ (1**, **2**) and Spectroscopic Characterization of Resultant Hexahydrides (**3**, **4**).** Reaction of **1** and **2** with HSbF_6 (65% aqueous solution) in benzene proceeds cleanly to afford the respective protonated complexes $[\text{ReH}_4(\eta^2\text{-H}_2)(\text{Cytpp})]\text{SbF}_6$ (**3**) and $[\text{ReH}_6(\text{ttpp})]\text{SbF}_6$ (**4**) in high yield. The corresponding BF_4^- salt of **3** can be prepared by using HBF_4 in place of HSbF_6 . Complexes **3** and **4** are air-stable solids that are remarkably resistant to loss of H_2 . For example, they remain intact after storage at 0.1 Torr for more than 2 days at ambient temperature. This behavior stands in contrast to that of $[\text{ReH}_6(\text{PR}_3)_3]^+$ ($\text{R}_3 = \text{Ph}_3$, Me_2Ph), obtained by protonation of $\text{ReH}_5(\text{PR}_3)_3$;^{21,29} for the latter, loss of H_2 occurs spontaneously at room temperature. However, the stability of **3** and **4** is similar to that reported for $[\text{ReH}_6(\text{etp})]^+$.^{7d} Complex **3** does not react with CO, N_2 , $t\text{-BuNC}$, or $\text{P}(\text{OMe})_3$ within 12 h in benzene at room temperature, or with D_2 within 2 h under UV irradiation at ambient temperature. However, it undergoes hydrogen/deuterium exchange upon treatment with D_2O in benzene- d_6 at ca. 25 °C. It can be deprotonated to **1** with NaO_2CH , NaO_2CMe , PMe_3 , or NEt_3 within 30 min in acetone at room temperature. Complex **4** does not react with CO and is deprotonated to **2** with NEt_3 under similar conditions.

The $^{31}\text{P}\{^1\text{H}\}$ NMR spectra of **3** and **4** (Table 2) consist of a doublet for the wing phosphorus atoms and a triplet for the central phosphorus atom as observed for **1** and **2**. The corresponding ^1H NMR spectra show a quartet pattern in the

(22) Inequivalent triangulated dodecahedral vertices are labeled A and B as shown, for example, in: Cotton, F. A.; Wilkinson, G. *Advanced Inorganic Chemistry*, 5th ed.; Wiley, New York, 1988; p 16.

(23) Cotton, F. A.; Luck, R. L. *J. Am. Chem. Soc.* **1989**, *111*, 5757.
 (24) Rhodes, L. F.; Huffman, J. C.; Caulton, K. G. *J. Am. Chem. Soc.* **1983**, *105*, 5137.
 (25) Meakin, P.; Guggenberger, L. J.; Peet, W. G.; Muettterties, E. L.; Jesson, J. P. *J. Am. Chem. Soc.* **1973**, *95*, 1467.
 (26) Teller, R. G.; Carroll, W. E.; Bau, R. *Inorg. Chim. Acta* **1984**, *87*, 121.
 (27) Abrahams, S. C.; Ginsberg, A. P.; Knox, K. *Inorg. Chem.* **1964**, *3*, 558.
 (28) Bau, R.; Carroll, W. E.; Hart, D. W.; Teller, R. G.; Koetzle, T. F. *J. Am. Chem. Soc.* **1977**, *99*, 3872.
 (29) Moehring, G. A.; Walton, R. A. *J. Chem. Soc., Dalton Trans.* **1987**, 715.

Table 2. Selected ^1H and $^{31}\text{P}\{^1\text{H}\}$ NMR Data for Complexes **1–12** at Ambient Temperature

compound	^1H NMR					$^{31}\text{P}\{^1\text{H}\}$ NMR		
	δ_{ReH}^a	J_{PcH}^b	J_{PwH}	δ_{CH} or δ_{CH_3}	$^4J_{\text{PcH}}$	δ_{Pc}^c	δ_{Pw}	J_{PcPw}
$\text{ReH}_5(\text{Cytpt})$, 1 ^d	-7.66 (td)	13.7	19.4			1.80 (t)	24.17 (d)	15.1
$\text{ReH}_5(\text{ttp})$, 2 ^d	-5.93 (td)	12.3	19.9			-8.53 (t)	11.34 (d)	15.0
$[\text{ReH}_4(\eta^2\text{-H}_2)(\text{Cytpt})]\text{SbF}_6$, 3 ^e	-6.06 (q)	15.3	15.3			-4.81 (t)	13.29 (d)	22.1
$[\text{ReH}_6(\text{ttp})]\text{SbF}_6$, 4 ^e	-4.47 (q)	14.0	14.0			-12.23 (t)	-4.03 (d)	21.8
$\text{ReH}_4(\text{SCH}=\text{S})(\text{Cytpt})$, 5 ^d	-2.64 (dt)	27.8	12.6	12.39 (d)	4.9	4.56 (t)	11.82 (d)	14.2
$\text{ReH}_4(\text{SCH}=\text{NC}_6\text{H}_4\text{NO}_2\text{-}p)(\text{Cytpt})$, 6 ^e	-3.46 (dt)	29.4	14.6	9.09 (s)		11.62 (br s)	13.38 (d)	14.1
$\text{ReH}_4(\text{SCH}=\text{NC}(\text{O})\text{OEt})(\text{Cytpt})$, 7 ^d	-3.06 (dt)	29.5	13.1	10.50 (d)	3.8	9.11 (t)	13.14 (d)	14.5
$\text{ReH}_4\text{I}(\text{Cytpt})$, 8 ^d	-2 (br), -4.21 (dt), -10 (br)	32.9	12.5			12.09 (t)	8.32 (d)	15.0
$[\text{ReH}_4(\text{MeCN})(\text{Cytpt})]\text{BF}_4$, 9 ^e	-2.92 (dt), -4.85 (br)	29.6	12.5	2.08 (s)		12.19 (t)	12.98 (d)	13.7
$[\text{ReH}_4(t\text{-BuNC})(\text{Cytpt})]\text{BF}_4$, 10 ^e	-5.29 (dt) ^f , -5.89 (q)	25.7, 19.2	14.2, 19.2	1.48 (s)		-1.27 (t)	10.56 (d)	15.8
$[\text{ReH}_4(\text{CyNC})(\text{Cytpt})]\text{BF}_4$, 11 ^e	-5.21 (dt), -5.77 (q)	25.3, 19.7	13.9, 19.7			-0.82 (t)	11.20 (d)	16.2
$[\text{ReH}_4\{\text{P}(\text{OMe})_3\}(\text{Cytpt})]\text{BF}_4$, 12 ^d	-5.78, -6.16, -6.57 (m) ^h			3.81(d) ^g		-10.15 (dt)	10.57 (t)	16.5

^a ^1H chemical shifts are in ppm with respect to Me_4Si (δ 0.0). Abbreviations: s = singlet, d = doublet, t = triplet, q = quartet, m = multiplet, and br = broad. ^b Coupling constants are in Hz. P_c is the central phosphorus atom and P_w are the wing phosphorus atoms in Cytpt and ttp ligands. ^c ^{31}P chemical shifts are in ppm with respect to external 85% H_3PO_4 (δ 0.0). ^d In C_6D_6 . ^e In CD_2Cl_2 . ^f $^2J_{\text{HH}} = 7.5$. ^g $^3J_{\text{PH}} = 11.1$. ^h Overlapping signals.

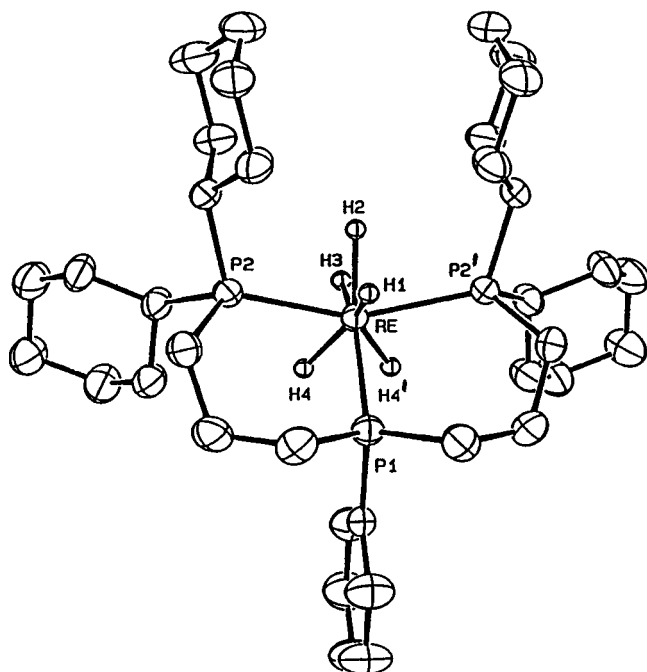


Figure 2. ORTEP drawing of **1** showing the atom-numbering scheme. Non-hydrogen atoms are represented by 50% probability thermal ellipsoids. Hydrogen atoms bonded to Re are drawn with an arbitrary radius; other hydrogen atoms are omitted for clarity.

Table 3. Selected Bond Distances (Å) and Angles (deg) for **1**

Bond Distances			
Re–P1	2.374(1)	Re–H2	1.60(5)
Re–P2	2.3828(7)	Re–H3	1.70(5)
Re–H1	1.62(5)	Re–H4	1.53(4)
Bond Angles			
P1–Re–P2	95.10(2)	P2–Re–H4	72(1)
P2–Re–P2'	151.80(4)	H1–Re–H2	68(2)
P1–Re–H1	71(2)	H1–Re–H3	141(3)
P1–Re–H2	139(2)	H1–Re–H4	137(2)
P1–Re–H3	148(2)	H2–Re–H3	73(3)
P1–Re–H4	73(2)	H2–Re–H4	132(2)
P2–Re–H1	79.2(3)	H3–Re–H4	73(2)
P2–Re–H2	77.5(2)	H4–Re–H4'	64(3)
P2–Re–H3	92.6(4)		

metal hydride region, which is indicative of fluxional behavior. When a CD_2Cl_2 solution of **3** is cooled to 183 K, this signal separates into three broad peaks centered at δ -5.31, -6.36, and -7.39 with relative intensities 1:4:1. The corresponding spectrum at 500 MHz shows some separation of the resonance

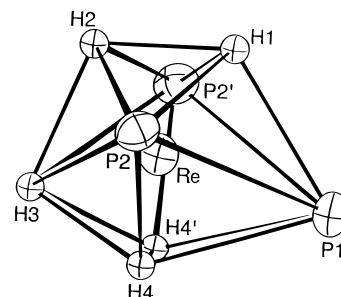


Figure 3. Arrangement of Re and eight ligand donor atoms in **1** emphasizing a triangulated dodecahedral structure.

at δ -6.36 into two peaks; the broader, featureless component ($\omega_{1/2} = 100$ Hz) at $\delta \sim -6.4$ may be due to $\eta^2\text{-H}_2$.³⁰ On the basis of T_1 measurements (T_1 (min) = 27 ms at 233 K, 250 MHz), presented in some detail in our communication,^{7f} complex **3** has been formulated as nonclassical. However, as pointed out by Crabtree and Luo^{7d} in scrutinizing corresponding data on $[\text{ReH}_6(\text{etp})]^+$, a minimum T_1 value of this magnitude does not unequivocally rule out a classical formulation. A nonclassical structure of **3** is, however, supported by an X-ray diffraction analysis of this complex in the solid (*vide infra*). Unlike for **3**, a limiting low-temperature ^1H NMR spectrum could not be obtained for **4**; only a broad, featureless signal was observed. The minimum T_1 value of 19 ms at 203 K (250 MHz) suggests that **4**, like **3**, is a nonclassical polyhydride.

The change from a classical to a nonclassical polyhydride upon protonation of **1** to **3** and, probably, **2** to **4** can be rationalized by the magnitude of metal $d\pi$ back-bonding into the σ^* orbital of H_2 . As the positive charge on the metal increases, the extent of this π bonding decreases to favor the presence of an $\eta^2\text{-H}_2$ ligand rather than two hydride ligands. Several examples of such a behavior are found in the literature.^{7d,31–33}

Description of the Structure of $[\text{ReH}_4(\eta^2\text{-H}_2)(\text{Cytpt})]\text{SbF}_6$ (3**).** An ORTEP drawing of the cation of **3** is given in Figure 4, and selected bond distances and angles are listed in Table 4. The overall geometry about the Re atom is that of a distorted triangulated dodecahedron (Re is 0.08 Å out of the plane defined

- (30) Kubas, G. J.; Unkefer, C. J.; Swanson, B. I.; Fukushima, E. *J. Am. Chem. Soc.* **1986**, *108*, 2547.
 (31) Crabtree, R. H.; Lavin, M.; Bonnevoit, L. *J. Am. Chem. Soc.* **1986**, *108*, 4032.
 (32) Morris, R. H.; Sawyer, J. F.; Shiralian, M.; Zubkowski, J. D. *J. Am. Chem. Soc.* **1985**, *107*, 5581.
 (33) Conroy-Lewis, F. M.; Simpson, S. J. *J. Chem. Soc., Chem. Commun.* **1986**, 506; **1987**, 1675.

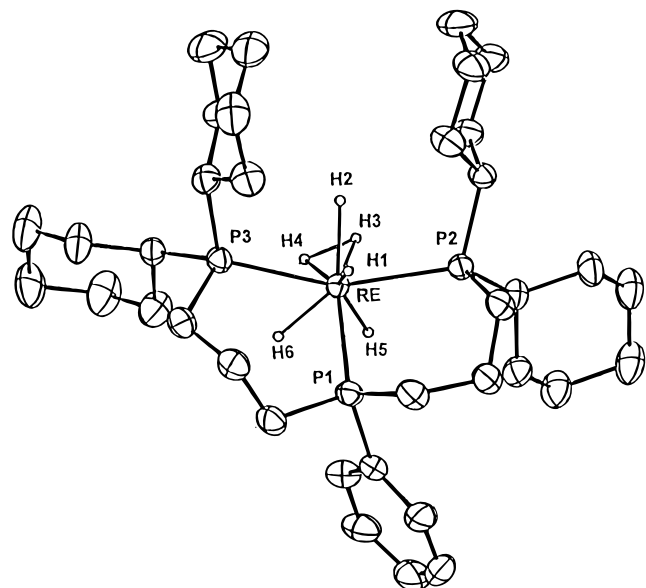


Figure 4. ORTEP drawing of the cation of **3** showing the atom-numbering scheme. Non-hydrogen atoms are represented by 50% probability thermal ellipsoids. Hydrogen atoms bonded to Re are drawn with an arbitrary radius; other hydrogen atoms are omitted for clarity.

Table 4. Selected Bond Distances (Å) and Angles (deg) for **3**

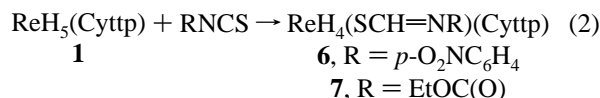
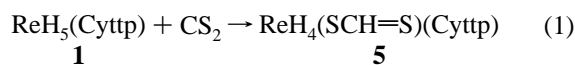
Bond Distances			
Re–P1	2.4300(7)	Re–H3	1.55(4)
Re–P2	2.4352(7)	Re–H4	1.45(3)
Re–P3	2.4400(7)	Re–H5	1.73(4)
Re–H1	1.63(3)	Re–H6	1.68(3)
Re–H2	1.68(3)	H3–H4	1.08(5)
Bond Angles			
P1–Re–P2	89.90(2)	P3–Re–H5	131(1)
P1–Re–P3	95.73(2)	P3–Re–H6	67(1)
P2–Re–P3	147.28(2)	H1–Re–H2	72(1)
P1–Re–H1	71(1)	H1–Re–H3	127(2)
P1–Re–H2	143(1)	H1–Re–H4	143(2)
P1–Re–H3	150(2)	H1–Re–H5	144(2)
P1–Re–H4	138(1)	H1–Re–H6	126(2)
P1–Re–H5	83(1)	H2–Re–H3	60(2)
P1–Re–H6	73(1)	H2–Re–H4	77(2)
P2–Re–H1	74(1)	H2–Re–H5	128(2)
P2–Re–H2	77(1)	H2–Re–H6	133(2)
P2–Re–H3	77(2)	H3–Re–H4	42(2)
P2–Re–H4	118(2)	H3–Re–H5	69(2)
P2–Re–H5	82(1)	H3–Re–H6	103(2)
P2–Re–H6	145(1)	H4–Re–H5	72(2)
P3–Re–H1	77(1)	H4–Re–H6	65(2)
P3–Re–H2	79(1)	H5–Re–H6	66(2)
P3–Re–H3	110(2)	Re–H3–H4	64(3)
P3–Re–H4	78(1)	Re–H4–H3	74(3)

by P1, H1, and H2) and closely resembles that of **1** (cf. Figure 2), with the hydride H3 having been replaced by η^2 -H₂ (H3H4). (The reader is alerted to the different atom-numbering schemes for **1** and **3** (cf. Figures 2 and 4)). This structure correctly predicts four different hydride resonances with relative intensities 1:2:2:1 in the low-temperature ¹H NMR spectrum of **3**.

The mean Re–P bond distance of **3** (2.435 Å) is longer than that of **1** and related rhenium pentahydrides, while the P–C bond distances (1.842(3) Å mean) decrease slightly in comparison to those of **1** (1.854(3) Å mean). The foregoing data are consistent with the recent proposal³⁴ of the participation of the σ^* orbitals of P–C in PR₃ as π -acceptors of metal electrons in back-bonding. The P–Re–P bond angles of **3** show a one

large/two small pattern (147.28(2), 89.90(2), 95.73(2)°) as expected for a triangulated dodecahedral structure. Although the Re–H bond distances (1.45(3)–1.73(4) Å) display a much wider range of values than those of **1**, the mean Re–H distance in **3** (1.62 Å) is similar to that in **1** (1.60 Å). The short H3–H4 bond distance of 1.08(5) Å³⁵ indicates the presence of an η^2 -H₂ ligand in the cation. The next shortest distance, H2···H3 (1.61(5) Å), is more consistent with a nonbonding interaction. In an attempt to obtain a more accurate structure of **3**, we tried to grow crystals suitable for a neutron diffraction study; however, our efforts were unsuccessful.

Insertion Reactions of ReH₅(Cyttp) (1**) with the Heterocumulenes X=C=S (X = S, *p*-O₂NC₆H₄N, EtOC(O)N).** The pentahydride **1** reacts at room temperature with CS₂ and RNCS (R = *p*-O₂NC₆H₄ and EtOC(O)) to afford insertion products containing dithioformate ligand and N-substituted thioformamide ligands, respectively, as shown in eqs 1 and 2. Selected ¹H and ³¹P{¹H} NMR data for the reaction products are given in Table 2.



The addition of CS₂ to **1** results in the formation of a yellow solid, ReH₄(SCH=S)(Cyttp) (**5**), characterized by analytical and spectroscopic data. In the ¹H NMR spectrum of **5**, the dithioformate resonance appears as a doublet at δ 12.39 with a ⁴J_{PH} = 4.9 Hz. Protons associated with dithioformate attached to metal in a monodentate or a bidentate mode resonate in the region δ 13.55–7.88.³⁶ The high-field region of the ¹H NMR spectrum of **5** at room temperature shows hydride resonances at δ –2.64 as an overlapping doublet of triplets and at ca. δ –6.0 as a broad peak owing to fluxionality. When the solution is cooled to 183 K, two signals are observed: a triplet at δ –3.2 and a multiplet at δ –8.3 with relative intensities 3:1, respectively. This defines the complex as a tetrahydride and strongly suggests that the coordination mode of S₂CH is through only one sulfur atom to satisfy the 18-electron rule. The ³¹P{¹H} NMR spectrum at 183 K shows an AX₂ splitting pattern: a doublet at ca. δ 11.5 for the two wing phosphorus atoms and a triplet at ca. δ 6.2 for the central phosphorus atom. The equivalence of the wing phosphorus atoms points to the presence of a plane of symmetry in the rigid structure in solution.

The IR spectrum of **5** in Nujol mull shows medium-intensity $\nu(\text{ReH})$ absorptions at 1965, 1945(sh), and 1935 cm^{–1}, as well as three strong-intensity absorptions at 1243, 1015, and 1005 (sh) cm^{–1} which may be assigned to $\nu_{\text{asym}}(\text{S}_2\text{CH})$ and $\nu_{\text{sym}}(\text{S}_2\text{CH})$, respectively. These strong bands are absent in the spectrum of **1**. Their frequencies are comparable to those reported for *trans*-PtH(SCH=S)[P(C₆H₁₁)₃]₂ (1240 and 1005 cm^{–1}), which was characterized by X-ray diffraction techniques and shown to contain a monodentate dithioformate ligand.^{36d}

The isothiocyanates RNCS (R = *p*-O₂NC₆H₄ and EtOC(O)) insert into one Re–H bond of **1** to afford violet and rust-colored solids, formulated as the S-bonded N-substituted thioform-

(34) (a) Orpen, A. G.; Connelly, N. G. *J. Chem. Soc., Chem. Commun.* **1985**, 1310. (b) Pacchioni, G.; Bagus, P. S. *Inorg. Chem.* **1992**, *31*, 4391.

(35) This distance may be compared with that of 1.06 Å calculated for the one-electron H₂⁺ ion; see: Schaad, J. L.; Hicks, W. V. *J. Chem. Phys.* **1970**, *53*, 851.

(36) (a) Harris, R. O.; Hota, N. K.; Sadavoy, L.; Yuen, J. M. C. *J. Organomet. Chem.* **1973**, *54*, 259. (b) Robinson, S. D.; Sahajpal, A. *J. Organomet. Chem.* **1975**, *99*, C65. (c) Robinson, S. D.; Sahajpal, A. *Inorg. Chem.* **1977**, *16*, 2718. (d) Albinati, A.; Musco, A.; Carturan, G. *Inorg. Chim. Acta* **1976**, *18*, 219.

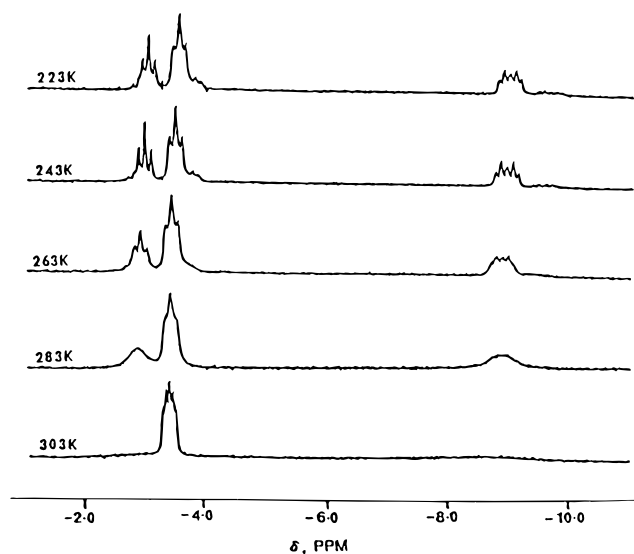


Figure 5. Variable-temperature ^1H NMR spectra of **6** in CD_2Cl_2 in the metal-hydride region.

amidate ($\text{Re}-\text{SCH}=\text{NR}$) complexes **6** and **7**, respectively (eq 2). Spectroscopic data of these products show similarities to those of **5**. Thus, the ^1H NMR spectra of **6** and **7** reveal a characteristic low-field signal of relative intensity 1 at δ 9.09 and 10.50, respectively. This signal is in the range reported for metal N-substituted thioformamidate complexes.³⁷ The presence of a thioformamidate ligand is also supported by the singlet resonances of CH at δ 160.63 and 163.61 in the $^{13}\text{C}\{^1\text{H}\}$ NMR spectra of **6** and **7**, respectively.

The high-field ^1H NMR spectrum of **6** at room temperature shows what appears to be an overlapping doublet of triplets centered at ca. δ -3.5. Upon cooling the solution to 283 K, two broad resonances grow in at ca. δ -2.9 and -8.9, and the room-temperature pattern at ca. δ -3.5 is now observed as an apparent triplet at δ -3.46. Further cooling to 243 K yields a spectrum that consists of two triplets, at δ -3.08 ($^2J_{\text{PH}} = 26.6$ Hz) and -3.58 ($^2J_{\text{PH}} = 25.8$ Hz), and an overlapping doublet of triplets at δ -8.96 ($^2J_{\text{PCH}} = 50.8$ Hz, $^2J_{\text{PWH}} = 28.9$ Hz) with relative intensities 1:2:1, respectively. These spectra are shown in Figure 5. The $^{31}\text{P}\{^1\text{H}\}$ NMR spectrum of **6** at ambient temperature consists of a broad signal at δ 11.62 of the central phosphorus atom and a doublet at δ 13.38 of the wing phosphorus atoms. Variable-temperature ^1H NMR spectra of **7** in the hydride region are similar to those of **6**. However, the limiting low-temperature spectrum at 243 K shows two overlapping triplets of different intensity centered at ca. δ -2.8 and an overlapping doublet of triplets at ca. δ -8.6. These signals integrate for 3 and 1 hydrogens, respectively. The $^{31}\text{P}\{^1\text{H}\}$ NMR spectra of **7** show no change in the AX_2 splitting pattern over the same temperature range.

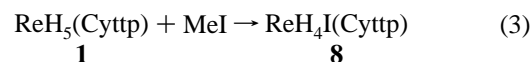
The foregoing high-field ^1H NMR spectra of **6** and **7** demonstrate that the two complexes are tetrahydrides. The electron count at metal then indicates that the thioformamidate ligand, like the thioformate ligand in **5**, is bonded in a monodentate fashion. The presence of three kinds of inequivalent hydride ligands in **6** is consistent with a triangulated dodecahedral structure of these molecules (cf. Figure 3: the thioformamidate ligand replaces H3). The proposed distribution of eight donor atoms in this structure places four small hydride ligands in the more crowded, four-neighbor A sites. The same polyhedral arrangement is probably also adopted by **5**; however, one of the two inequivalent hydrogens (H1 or H2) has the same

chemical shift as the equivalent pair (H4 and H4'; all hydrogen numbering is that given in Figure 3). The $^{31}\text{P}\{^1\text{H}\}$ NMR spectra of **5**–**7** are consistent with this arrangement of ligands.

Upon close examination of the low-temperature ^1H NMR spectra of **6**, it is evident that a second complex is present in solution. This minor species (ca. 1:7.8 ratio) shows resonances with the chemical shifts very close to those of the major complex. Additionally, at 243 K a signal is observed at δ 9.32 which appears to be due to the *N*-arythioformamidate CH proton of the minor species. The $^{31}\text{P}\{^1\text{H}\}$ NMR spectrum at 243 K also clearly shows the presence of the minor product. All of this spectroscopic behavior is reversed upon increasing the temperature.

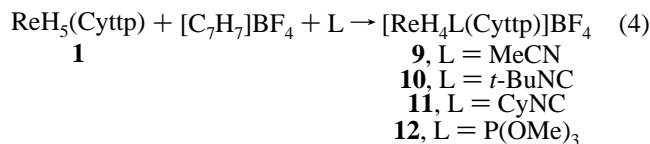
We think that the most plausible explanation of these results is in terms of an equilibrium between two similar species, probably the isomers containing the S-bonded and the N-bonded ($\text{Re}-\text{N}(\text{R})\text{CH}=\text{S}$) *N*-arythioformamidate ligand. The major isomer is most likely the S-bonded one, since in this structure the relatively bulky *p*- $\text{O}_2\text{NC}_6\text{H}_4$ group avoids the chelating phosphine ligand. N-substituted thioformamidate ligands are known to bind to metal through both nitrogen and sulfur.³⁷

Reactions of $\text{ReH}_5(\text{Cytpt})$ (1**) with MeI and $[\text{C}_7\text{H}_7]\text{BF}_4$ in the Presence of L (L = MeCN, *t*-BuNC, CyNC, $\text{P}(\text{OMe})_3$).** The reaction of **1** with MeI gives a white solid, $\text{ReH}_4\text{I}(\text{Cytpt})$ (**8**) (eq 3), in high yield. Selected ^1H and $^{31}\text{P}\{^1\text{H}\}$ NMR data



for **8** and a number of complexes $[\text{ReH}_4\text{L}(\text{Cytpt})]\text{BF}_4$ are presented in Table 2. The ambient-temperature ^1H NMR spectrum of **8** in the hydride region shows a multiplet at δ -4.21 of relative intensity 2 and two broad signals at ca. δ -2 and -10. This spectrum differs from the ambient-temperature hydride-region ^1H NMR spectrum of a monophosphine analogue of **8**, $\text{ReH}_4\text{I}(\text{PPh}_3)_3$,³⁸ which shows a quartet of relative intensity 4. When a solution of **8** is cooled to 240 K, three sharp resonances are obtained: two triplets, at δ -2.23 ($^2J_{\text{PH}} = 27.9$ Hz) and -4.34 ($^2J_{\text{PH}} = 27.5$ Hz), and a multiplet at δ -10.48 with relative intensities 1:2:1, respectively. This spectrum is remarkably similar to that of **6** and suggests a comparable triangulated dodecahedral structure for **8**. The $^{31}\text{P}\{^1\text{H}\}$ NMR spectrum is consistent with this arrangement of ligands.

Complex **1** reacts with $[\text{C}_7\text{H}_7]\text{BF}_4$ in the presence of various ligands L to afford the tetrahydrides **9**–**12** (eq 4). In these



reactions, $[\text{C}_7\text{H}_7]^+$ behaves as a hydride-ion abstractor to generate a coordinatively unsaturated Re complex which combines with L. Similar reactions of $[\text{C}_7\text{H}_7]\text{PF}_6$ and monodentate ligands L with $\text{ReH}_5(\text{PPh}_3)_3$ afforded a series of complexes $[\text{ReH}_4\text{L}(\text{PPh}_3)_3]\text{PF}_6$.²⁹ The ^1H NMR spectra of **9**–**11** at room temperature show two hydride resonances of equal intensity (total intensity 4); this may be contrasted with the appearance of only one signal in the spectra of the analogous complexes $[\text{ReH}_4\text{L}(\text{PPh}_3)_3]\text{PF}_6$.²⁹ The $^{31}\text{P}\{^1\text{H}\}$ NMR spectra give the expected AX_2 pattern. The presence of the MeCN ligand in **9** is indicated by the signals in the ^1H NMR spectrum

(38) (a) Freni, M.; Giusto, D.; Romiti, P.; Zucca, E. *J. Inorg. Nucl. Chem.* **1969**, *31*, 3211. (b) Allison, J. D.; Moehring, G. A.; Walton, R. A. *J. Chem. Soc., Dalton Trans.* **1986**, 67.

(37) Robinson, S. D.; Sahajpal, A. *Inorg. Chem.* **1977**, *16*, 2722.

at δ 2.08 and in the $^{13}\text{C}\{^1\text{H}\}$ NMR spectrum at δ 126.6 (doublet, $^3J_{\text{PC}} = 5.6$ Hz, CN) and 3.95 (singlet, Me). The IR spectra of **10** and **11** contain strong absorption bands at 2160 and 2170 cm^{-1} , respectively, which are assigned to $\nu(\text{CN})$ of the isonitrile ligand.

The room-temperature ^1H NMR spectrum of **12** shows hydride resonances at δ -5.78, -6.16, and -6.57 with the combined intensity of 4. The presence of $\text{P}(\text{OMe})_3$ is indicated by the appearance of a doublet signal at δ 3.81 ($^3J_{\text{PH}} = 11.1$ Hz). In the $^{31}\text{P}\{^1\text{H}\}$ NMR spectrum, the resonance of $\text{P}(\text{OMe})_3$ is observed at δ 120.85 as a doublet of triplets with $^2J_{\text{PcP}} = 91.2$ Hz and $^2J_{\text{PwP}} = 17.2$ Hz. The former coupling constant suggests a large bond angle $\text{Pc}-\text{Re}-\text{P}(\text{OMe})_3$. The central and the wing phosphorus atoms of Cyttp resonate at δ -10.15 and 10.57 as a doublet of triplets and a triplet ($^2J_{\text{PcPw}} = 16.5$ Hz), respectively. Altogether these spectroscopic data suggest a structure similar to that proposed for the other tetrahydride complexes prepared herein.

It is noteworthy that the chemical shift of the central phosphorus atom (Pc) of the Cyttp ligand is sensitive to the nature of L (cf. Table 2). Thus, δ_{Pc} of **9**, with a weak ligand, MeCN, occurs at a lower field (12.19 ppm) than δ_{Pc} of **10–12**, containing strong ligands, *t*-BuNC, CyNC, and $\text{P}(\text{OMe})_3$ (-1.27 to -10.15 ppm), respectively. In contrast, the chemical shift of the wing phosphorus atoms (Pw) is essentially invariant to L. This trend provides support for the proposed triangulated dodecahedral structures in which L is "trans" to Pc (i.e. a large $\text{Pc}-\text{Re}-\text{L}$ bond angle, position H3 in Figure 3). (Occupancy of position H2 in Figure 3 by L would also result in a large $\text{Pc}-\text{Re}-\text{L}$ bond angle. However, ligand L would be more crowded in this position than in position H3.)

Conclusions

The pentahydride $\text{ReH}_5(\text{Cyttp})$ (**1**) was shown by X-ray diffraction techniques to adopt a classical, triangulated dodeca-

hedral structure in the solid. The three phosphorus atoms together with one hydrogen atom occupy the four five-neighbor B sites while the remaining hydrogen atoms occupy the four four-neighbor A sites of this polyhedron. Complex **1** displays a rich chemistry of the hydride ligand. Thus, it undergoes protonation by HSbF_6 to yield $[\text{ReH}_4(\eta^2\text{-H}_2)(\text{Cyttp})]\text{SbF}_6$ (**3**), which has a nonclassical hydride, triangulated dodecahedral structure in the solid. The same structure is suggested in solution by ^1H NMR measurements. Surprisingly, **3** is quite unreactive: it is resistant to loss of H_2 and is unaffected by CO, *t*-BuNC, or $\text{P}(\text{OMe})_3$ at ambient temperature. **1** inserts a molecule of each of the heterocumulenes CS_2 , *p*- $\text{O}_2\text{NC}_6\text{H}_4\text{NCS}$, and $\text{EtOC}(\text{O})\text{NCS}$ ($\text{X}=\text{C}=\text{S}$) to afford the tetrahydride products $\text{ReH}_4(\text{SCH}=\text{X})(\text{Cyttp})$ (**5–7**, respectively). It undergoes a $\text{Re}-\text{H}$ bond cleavage reaction with MeI to produce $\text{ReH}_4\text{I}(\text{Cyttp})$ (**8**) and a hydride abstraction/substitution reaction with $[\text{C}_7\text{H}_7]\text{BF}_4$ in the presence of L to yield $[\text{ReH}_4\text{L}(\text{Cyttp})]\text{BF}_4$ (L = MeCN (**9**), *t*-BuNC (**10**), CyNC (**11**), and $\text{P}(\text{OMe})_3$ (**12**)). All of the tetrahydride complexes **5–12** are stable, classical polyhydrides that appear to adopt a triangulated dodecahedral structure, with the hydrogens occupying the A sites and the other four donor atoms the B sites, as suggested by ^1H and $^{31}\text{P}\{^1\text{H}\}$ NMR data.

Acknowledgment. We thank the National Science Foundation (A.W.), The Ohio State University, and Korea Research Foundation (Non-directed Research Fund, Y.K., 1993) for support.

Supporting Information Available: Tables of complete information on collection of data and refinement of structure, all atomic coordinates with isotropic thermal parameters, anisotropic displacement coefficients; bond distances and angles, selected hydrogen-hydrogen nonbonding distances for **1** and **3**, and selected IR data for **9–12** (15 pages). Ordering information is given on any current masthead page.

IC9602714